Available online at www.sciencedirect.com

SciVerse ScienceDirect

Ceramics International 39 (2013) 2827–2834

CERAMICS INTERNATIONAL

www.elsevier.com/locate/ceramint

Direct and pulse current electrodeposition of Ni–W–TiO_2 nanocomposite coatings

K. Arunsunai Kumar, G. Paruthimal Kalaignan*, V.S. Muralidharan

Advanced Nano Composite Coatings Laboratory, Department of Industrial Chemistry, School of Chemical Sciences, Alagappa University, Karaikudi 630003, Tamilnadu, India

Received 9 July 2012; received in revised form 14 September 2012; accepted 14 September 2012
Available online 2 October 2012

Abstract

Ni–W–TiO_2 nanocomposite coatings have been obtained on mild steel surface by direct current (DC) and pulse current (PC) electrodeposition from Watts bath containing an ammonical citrate complexing agent. The morphology of the coatings was explored by scanning electron microscopy (SEM), atomic force microscopy (AFM) and the composition of the electrodeposits was analyzed by energy dispersive X-ray analysis (EDX). Surface morphology studies revealed that Ni–W alloy surface was covered by long needle like crystals and Ni–W–TiO_2 composite coatings with smaller spherical sized grains. The coated surface contained 25.55% W and 5.55% Ti. XRD studies revealed that (111) plane was predominant in both Ni–W alloy deposits and Ni–W–TiO_2 composite coatings. The patterns of the electrodeposits confirmed only fcc frame work structure. Microhardness values increased with TiO_2 addition in the alloy. The corrosion resistance of Ni–W alloy deposit and TiO_2 incorporated coatings was evaluated by Potentiodynamic polarization studies in 3.5% NaCl solutions. Corrosion current densities decreased with TiO_2 inclusion in the alloy deposit. Electrochemical impedance studies revealed that the charge transfer resistance increased with TiO_2 inclusion in the alloy deposits while the double layer capacitance decreased. The PC composites coatings offer uniform surface, high microhardness and enhanced corrosion resistance than DC composites coatings.

Keywords: B. Nanocomposites; Pulse electrodeposition; Surface morphology; Microhardness

1. Introduction

Electrodeposited composite coatings exhibited enhanced material properties such as a mechanical, electrochemical and oxidation properties compared to pure metal coatings. Improvement of these properties depended mainly on the size and the percentage of the electrodeposited particles [1]. Pulse plating offers a greater control over the structure and properties of electrodeposits than the conventional direct current plating [2]. Pulse current electrodeposited coatings have higher mechanical and tribological properties compared to direct current electrodeposits [3,4]. The composite coatings of nickel (Ni–Al_2O_3, Ni–SiC and Ni–ZrO_2) have been prepared and the amount of reinforcement in the coatings increased in the pulse current and pulse reverse current deposition compared to direct current [5]. The effect of pulse frequency, duty cycle and concentration of Si_3N_4 nanoparticles containing a nickel sulfate bath had been discussed [6]. Nano Ni–TiN coating was obtained using ultrasonic electrodeposition [7]. The Ni–Al_2O_3 composite coatings were prepared by DC, PC and PRC electrodeposition methods. The corrosion behavior of these electrodeposits at high temperatures was also investigated [8]. Electrochemical impedance spectroscopy was used to characterize the mechanism involved in the deposition of the nickel–cerium oxide coatings from the chloride baths [9]. The electrodeposition of Ni–SnO_2 composite coatings on steel substrates and the evaluation of mechanical properties had been reported [10]. TiO_2 co-deposition was carried out with Cu and Zn as the metallic components [11–13]. The co-deposition of TiO_2 particles in

*Corresponding author. Tel.: +91 9443135307; fax: +91 4565 225202.
E-mail addresses: arunsunai@gmail.com (K. Arunsunai Kumar), pkalaignan@yahoo.com (G. Paruthimal Kalaignan), varagur@yahoo.com (V.S. Muralidharan).

0272-8842/$ - see front matter Crown Copyright © 2012 Published by Elsevier Ltd and Techna Group S.r.l. All rights reserved.
http://dx.doi.org/10.1016/j.ceramint.2012.09.054

nickel matrix to improve the mechanical and corrosion properties had been investigated [14–19]. The Ni–TiO_2 composite coatings were prepared on steel substrates through electrodeposition and its mechanical properties had been reported [20].

The corrosion studies in 3.5 wt% NaCl solution at pH 3 and 10 for the reverse pulse electrodeposited nanocrystalline Ni–W alloys revealed that the corrosion rates of the alloys have increased with the reduction of grain size in alkaline solutions but decreased with in acidic solutions [21]. Corrosion resistance behavior of nanocrystalline Ni–W alloy coatings were electrodeposited using a direct and pulse current methods [22–26]. Various amounts of TiO_2 incorporation in Ni–P–TiO_2 nanocomposite coatings were electrodeposited on low carbon steel [27]. Direct, pulse and pulse reverse current electrodeposition of Ni–Co–Al_2O_3 composite coatings and the microstructure of the deposits had been discussed [28,29]. TiO_2 incorporation was carried out in Ni–Co alloy matrix. The microstructure and its corrosion property had been reported [30].

Direct current method was used to deposit Ni–W–SiC nanocomposite at high current density ranges from 6 to 18 A/dm^2 [31]. Ni–W–La_2O_3 coating was also prepared by direct current method. La_2O_3 addition refined the microstructure of Ni–W alloy and provided uniform elemental distribution [32]. CeF_3 was co-deposited with Ni–W alloy by direct current method to improve the tribological properties [33]. Pulse plating was used to incorporate nanosized Al_2O_3 particles in the Ni–W alloy [34]. MoS_2 particles were co-deposited with Ni–W using pulse plating to provide effective lubricative coatings [35]. Pulse current was used to get Ni–W–CNT nanocomposite coatings with more carbon nano tubes and uniform distribution of carbon nano tubes in the coatings [36]. The amount of CeO_2 present in the Ni–W coating and high temperatures tribological performances of the composite coating against molten glass were also investigated [37].

The present communication deals with the direct current and pulse current electrodeposition of Ni–W–TiO_2 nanocomposite coatings obtained from citrate complexed alkaline bath (pH 9). The electrodeposits were characterized for their surface morphology and surface structure using the scanning electron microscopy and XRD. Hardness measurements were also carried out on the electrodeposits. Corrosion resistance properties were evaluated by using electrochemical measurements in 3.5% NaCl solution at pH 7.

2. Experimental details

Cold rolled mild steel plates were polished with fine grid paper and degreased with trichloroethylene, then cathodically electrocleaned in alkaline solution for 2 min and anodically for 30 s in a solution mixture containing 35 g L^{-1} NaOH and 25 g L^{-1} Na_2CO_3 at 30 °C. They were washed in running water and then dipped in 5% H_2SO_4 solutions for 10 s. The current density applied for cathodic cleaning was 7 A/dm^2. Open circuit potential of the polished, pre cleaned steel specimens in the plating bath (pH = 9) was −540 mV vs SCE. After the application of cathodic current density, the potential of the steel became −1100 mV vs SCE.

Pulse and direct current electrodeposition was carried out using a Myriad Bipolar pulsed power supply (Shruthi Enterprises, Bangalore) was employed. Thus prepared mild steel plates of size 3 × 2.5 × 0.05 cm were used as cathodes. The pure nickel plate of size 4 × 2.5 × 0.4 cm was used as anode. All the chemicals used were of AnalaR Grade. Table 1 summarizes the suppliers of the chemicals and conditions of the electrodeposition. The titanium oxide (TiO_2) was crystalline and anatase with structure. The particle size of titanium dioxide was 200–500 nm. The hardness of the electrodeposits was measured by using MHG Everyone Hardness Tester (Hong Kong). The microhardness of the deposit in kg mm^{-2} was determined by using the formula

$$Hv = 1854 \times L/d^2 \quad (1)$$

where L is the load applied in g and d the diagonal of the indention (μm). The load applied was 50 g. Scanning electron microscope (SEM) (HITACHI S-570, Japan) was used to characterize the surface morphology of the composite coatings. For these studies, the electrodeposited panels were cut in to 1 cm × 1 cm size, cold mounted, examined and photographed. The deposited surface was subjected to EDAX (Energy Dispersive X-ray analysis) for the determination of chemical composition of the deposits. The crystalline structure of the plated substrate was identified by X-ray diffraction using Brooker D8 advance X-ray diffractometer operated with Cu Kα radiation (nickel filtered) was used at a rating of

Table 1
Composition and conditions of plating bath.

Chemicals	Source	Composition	Plating parameters
Nickel sulfate	Sigma-Aldrich	0.15 M	Pulse peak c.d. 1.5 Adm^{-2}
Sodium tungstate	Sigma-Aldrich	0.15 M	pH 9
Tri-ammonium citrate (TAC)	Sigma-Aldrich	0.30 M	Time 40 min
Ammonium chloride	SRL	0.20 M	Temperature 70 °C
Dimethyl sulphoxide (DMSO)	SRL	0.06 M	Constant stirring
Sodium lauryl sulfate (SLS)	Sigma-Aldrich	0.80 gL^{-1}	**Pulse Duty Cycle**
2-Butyne 1,4-diol (BD)	SRL	50 m gL^{-1}	On time: 40 ms
Anatase-(TiO_2)- 200–500 nm	Sigma-Aldrich	0–15 gL^{-1}	Off time: 30 ms

40 KV, 20 mA. The scan rate was 0.05 °C per step and the measuring time 15/step. The crystallite size was calculated by using the Scherrer equation [38].

$$D = \frac{0.9\lambda}{\beta \cos\theta} \quad (2)$$

where D is the crystallite size, λ is the incident radiation (1.5418 Å), β is the corrected peak width at half-maximum intensity and θ is the angular position. Electrochemical measurements were carried out using a three electrodes cell assembly. Electrodeposit of 1 cm^2 exposed area was used as a working electrode. A rectangular platinum foil and a saturated calomel electrode were used as auxiliary and reference electrodes respectively. The test solution was 3.5% NaCl kept at 30 °C. Electrochemical polarization studies were carried out by using Eco-chemie-Potentiostat galvanostat (Auto lab). Electrochemical impedance measurements were done on the electrodeposits after they attained steady corrosion potential. The impedance measurements were made in the frequency range of 10 Kc/s–10 mc/s with a sinusoidal perturbation of 10 mV.

3. Results and discussion

3.1. X-ray diffraction studies

X-ray diffraction patterns for Ni–W alloy as well as Ni–W–TiO_2 nanocomposites are shown in Fig. 1.These patterns revealed crystalline fcc structure of Ni–W alloy with predominant planes (111), (200) and (220). JCPDS standards (65-4828) have confirmed the patterns. The crystallite sizes of Ni–W and Ni–W–TiO_2 (DC, PC) nanocomposites were calculated using Scherrer equation. The crystallite sizes of (111) plane of electrodeposited Ni–W, Ni–W–TiO_2 (DC) and Ni–W–TiO_2 (PC) were found to be 102 nm, 80 nm and 72 nm respectively. Pulse electrodeposits had smaller crystals compared to direct current electrodeposited Ni–W–TiO_2 nanocomposite and Ni–W alloy coatings. The addition of TiO_2 decreased the crystallite sizes.

In an earlier study [23] the appearance of peaks at 51°, 60° and 90°, 2θ values in the diffractograms were related to (111), (200) and (220) planes of $Ni_{17}W_3$ alloy in the Ni–W electrodeposits. Only noticeable differences can be observed in the intensities of (111), (200) and (220) peaks for Ni–W–TiO_2 nanocomposite. The (111) peak intensity was greater than other planes suggesting the predominant (111) texture. The crystallite sizes were of the order of nm. The development of this texture was associated with the preferred growth along (111) orientation because of the lower strain associated

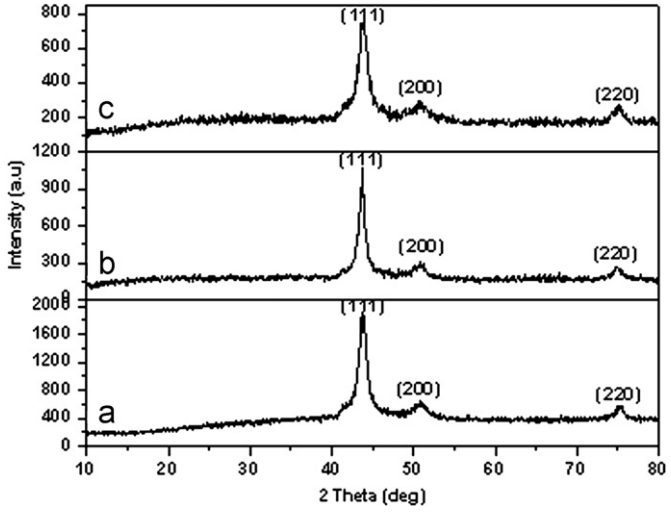

Fig.1. XRD Patterns observed for: (a) Ni–W alloy deposit (b) Ni–W–TiO_2 (DC) composite and (c) Ni–W–TiO_2 (PC) composite.

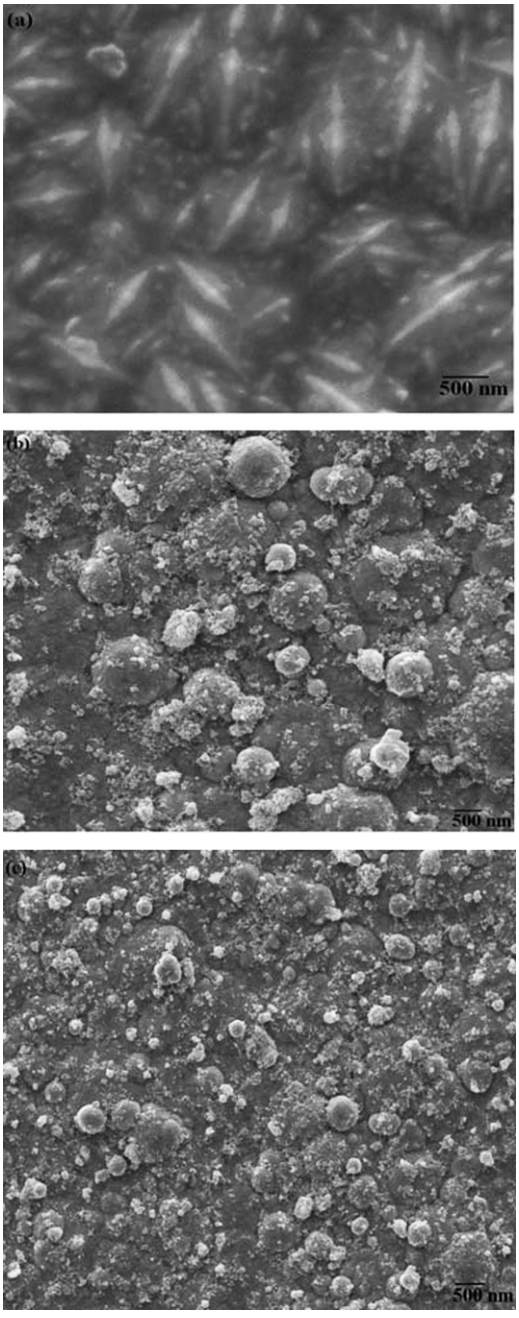

Fig. 2. SEM for electro: (a) deposit A (b) deposit D by DC method (C) deposit D by PC method.

in this direction. Broadened Bragg peaks were seen in the nanocomposites compared to Ni–W alloy deposit. This broadening was increased with addition of TiO_2 in the Ni–W alloy deposit. This is due to the reduction in crystallite size with TiO_2 addition. The formation of non-crystalline structure was not favoured as seen from the appearance of well-defined sharp peaks.

3.2. SEM and EDAX measurements

Surface morphologies of electrodeposits obtained under various conditions are shown in Fig. 2a–c. The needle shaped grain was seen on the surface of Ni–W alloy. Ni–W–TiO_2 nanocomposite surface obtained under DC and PC conditions were found to have smaller spherical shape grains. These suggest that TiO_2 particles were uniformly distributed in the alloy matrix. The composite deposits obtained from PC method exhibited smooth and smaller spherical shape grains compared to the nanocomposite surface obtained by the DC method. The EDAX spectra of the electrodeposits are shown in Fig. 3a–c. The EDAX analysis gives the % of elements present in the Ni–W–TiO_2 nanocomposite coatings (Table 2). The EDAX analysis reveals that oxygen content is less than that of corresponding TiO_2. Perhaps some of the surface TiO_2 particles might have undergone "catalytic reduction" to Ti by adsorbed nascent H_2 formed during electrodeposition. However, bulk deposit contained TiO_2 particle.

3.3. AFM measurements

Fig. 4a–c shows that the surface morphologies of electrodeposited Ni–W alloy and Ni–W–TiO_2 nanocomposite coatings were prepared by DC and PC methods. The pulse current electrodeposited Ni–W–TiO_2 nanocomposite coating surface had much smaller particle size. The co-deposited TiO_2 particles were uniformly distributed over the Ni–W alloy matrix. The presence of TiO_2 decreased the size of particles.

Table 2
EDAX analysis of Ni–W and Ni–W–TiO_2 nanocomposite coating.

Deposit	Elements	Amount of nanocomposite (%) $\pm$ 0.1
A	Ni	71.4
	W	28.5
D-DC	Ni	68.60
	W	26.45
	Ti	3.26
	O	1.58
D-PC	Ni	67.4
	W	25.01
	Ti	5.55
	O	1.88

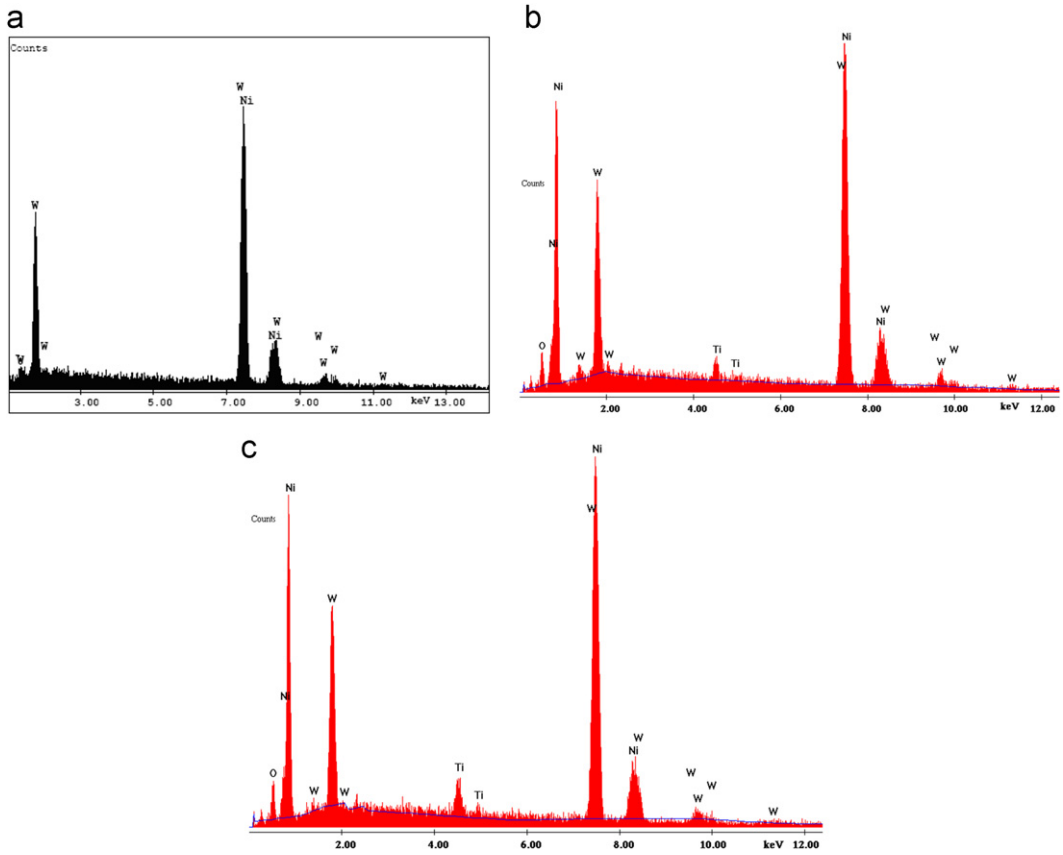

Fig. 3. EDAX spectrum for: (a) deposit A (b) deposit D by DC method (C) deposit D by PC method.

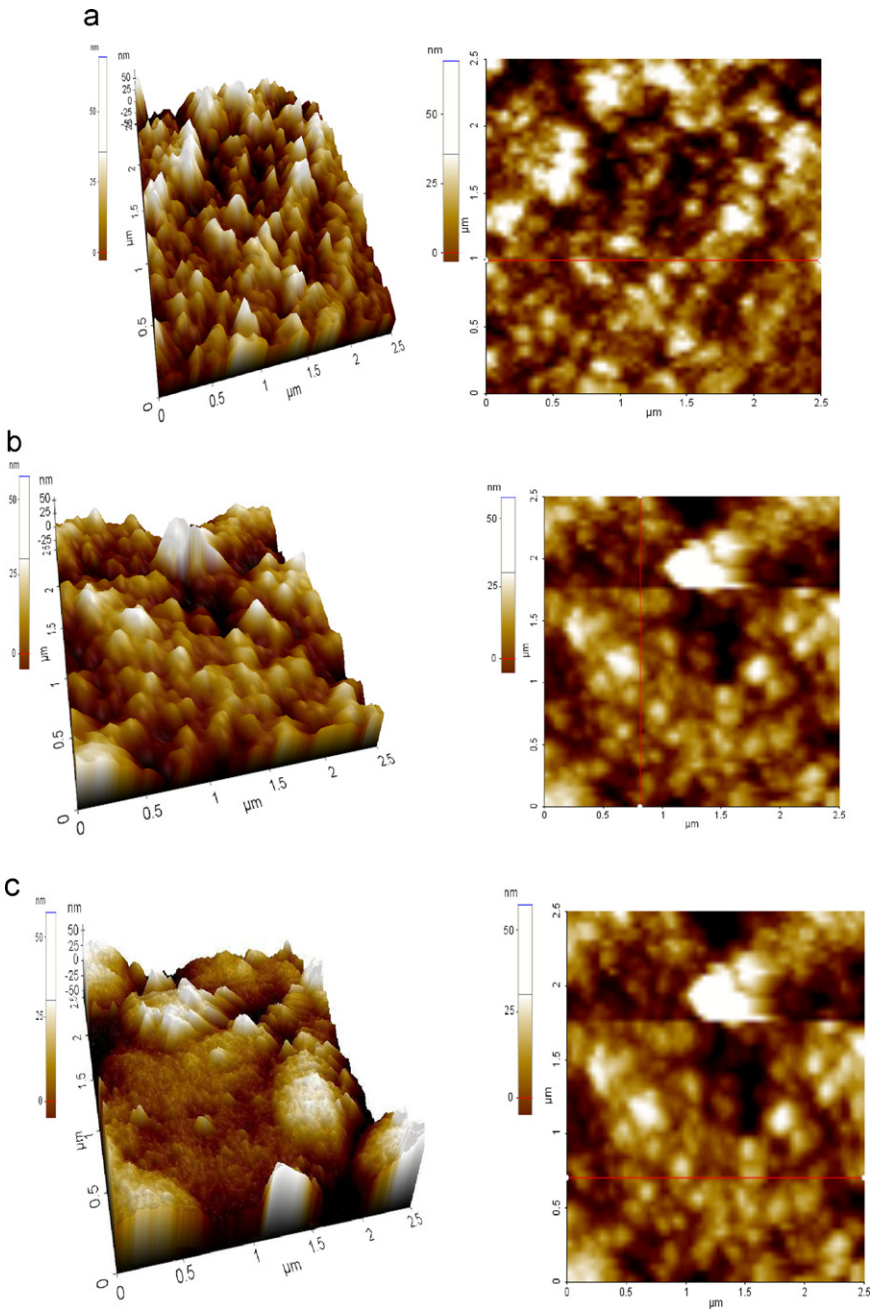

Fig. 4. (a) AFM images of Ni–W alloy deposit. (b) AFM images of Ni–W–TiO_2 deposit by DC method. (c) AFM images of Ni–W–TiO_2 deposit by PC method.

3.4. Microhardness test

Fig. 5 presents the microhardness values for various electrodeposits. Incorporation of TiO_2 particles in the alloy enhanced the microhardness. PC deposits offer enhanced microhardness compared to DC deposit. The microhardness values were varied from 467 to 686 Hv. The amount of TiO_2 present in the coating contributed to its higher hardness. The incorporation of TiO_2 had taken place on the metal layer by adsorption as suggested by Guglielmi's two-step adsorption model [39,40]. Increase in microhardness is due to (a) dispersive strengthening effect of TiO_2 (b) nanoparticles in the composite coatings blocking the dislocation motion and the grain boundary sliding of the matrix and (c) nanoparticles in the coatings restricted the growth of crystalline bulk in the process of electrodeposition. The PC composite had a finer grain size which caused lower porosity of the coating and greater compact structure.

3.5. Electrochemical characterizations

Corrosion resistances of the electrodeposits were evaluated in 3.5% NaCl solution by electrochemical methods. Fig. 6 presents the polarization curves obtained from potentiodynamic polarization method for various DC deposits. The linear segments of the anodic and cathodic

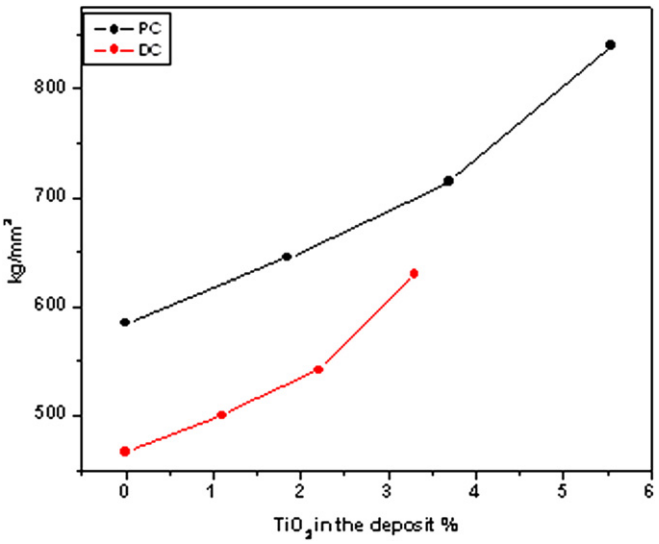

Fig. 5. Effect of the co-deposited TiO_2 on the microhardness of Ni–W–TiO_2 nanocomposite coatings.

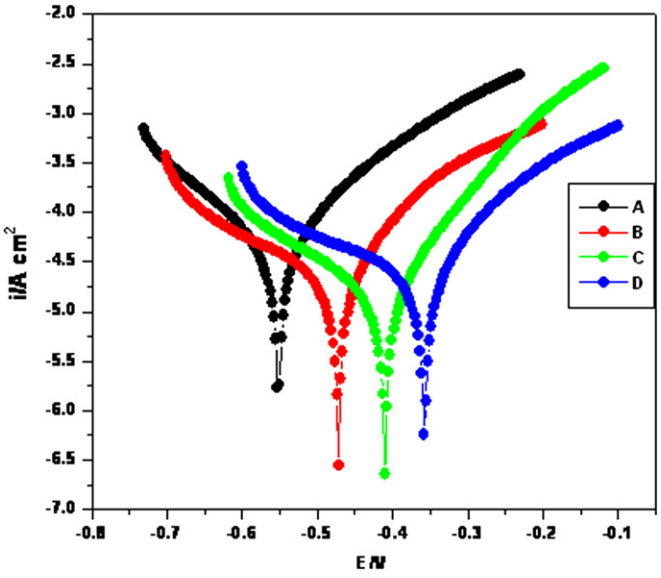

Fig. 6. Potentiodynamic polarization curves for Ni–W alloy deposit and for various amounts of TiO_2 incorporated in to Ni–W alloy deposit by DC Method.

Table 3
Parameters derived from potentiodynamic polarization curves for Ni–W deposit and Ni–W–TiO_2 nanocomposite coatings obtained using DC Method.

Deposit	TiO_2 in the deposit (wt%)	E_{corr} vs SCE (mV)	b_a (mV decade^{-1})	b_c (mV decade^{-1})	i_{corr} (μA cm^{-2})
A	0	−550	125	98	16.8
B	1.1	−471	96	103	13.7
C	2.2	−410	109	98	7.5
D	3.3	−358	121	73	5.4

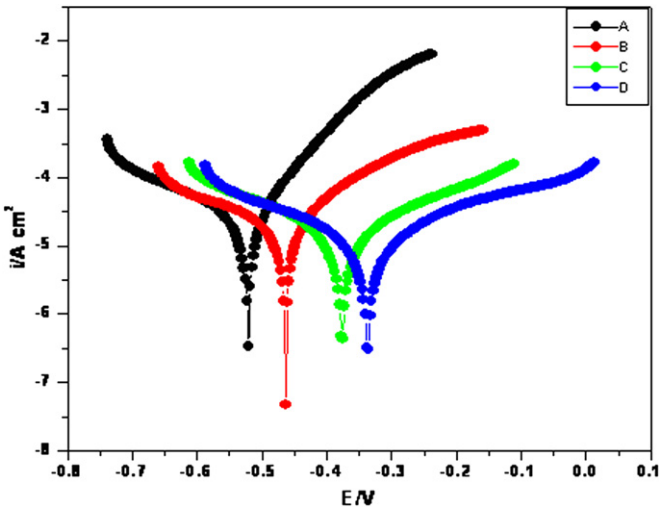

Fig. 7. Potentiodynamic polarization curves for Ni–W alloy deposit and for various amounts of TiO_2 incorporated in to Ni–W alloy deposit by PC Method.

Table 4
Parameters derived from potentiodynamic polarization curves for Ni–W deposit and Ni–W–TiO_2 nanocomposite coatings obtained using PC Method.

Deposit	TiO_2 in the deposit (wt%)	E_{corr} vs SCE (mV)	b_a (mV decade^{-1})	b_c (mV decade^{-1})	i_{corr} (μA cm^{-2})
A	0	−520	134	95	15.3
B	1.9	−463	63	113	7.5
C	3.7	−375	78	104	6.5
D	5.6	−335	62	73	3.2

curves were extrapolated to corrosion potential to calculate the corrosion current densities. The slopes of these linear segments were used to calculate Tafel slopes. Corrosion current density values decreased with the incorporation of TiO_2 (Table 3). Fig. 7 presents the potentiodynamic polarization curves obtained for various PC deposits. Corrosion current density values decreased with TiO_2 incorporation (Table 4).

The EIS spectra revealed the impedance information for the deposits exposed in corrosive solutions. Fig. 8 presents the Nyquist plots for Ni–W alloy deposit and Ni–W–TiO_2 nanocomposite coatings prepared by DC method. Charge transfer (R_{ct}) and double layer capacitance (C_{dl}) values were increased and decreased with TiO_2 incorporation respectively (Table 5). The Nyquist plots obtained for various deposits prepared by PC method are shown in Fig. 9. All the composite coatings offered increased R_{ct} values and decreased C_{dl} values with TiO_2 incorporation (Table 6). From the electrochemical theory of corrosion, corrosion current densities are inversely proportional to charge transfer resistance. Stern–Geary equation [41] relates

$$i_{corr} = \frac{1}{2.303 R_{ct}} \left[\frac{b_a b_c}{b_a + b_c} \right]$$

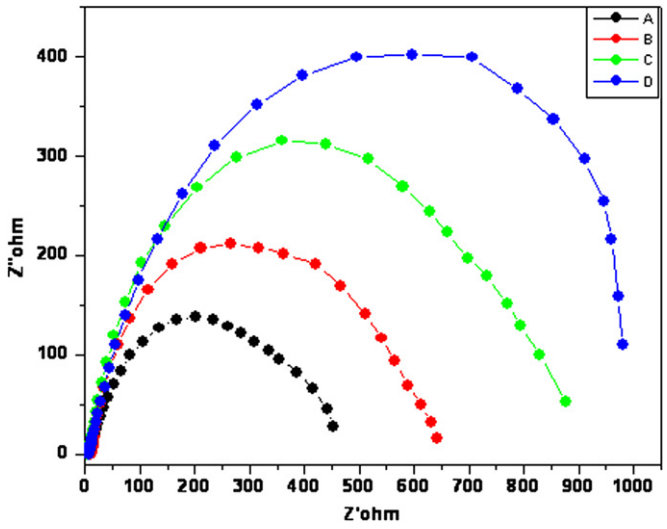

Fig. 8. Nyquist plots (Z''*vs* Z') obtained for Ni–W alloy deposit and for various amounts of TiO_2 incorporated in to Ni–W alloy deposit by DC Method.

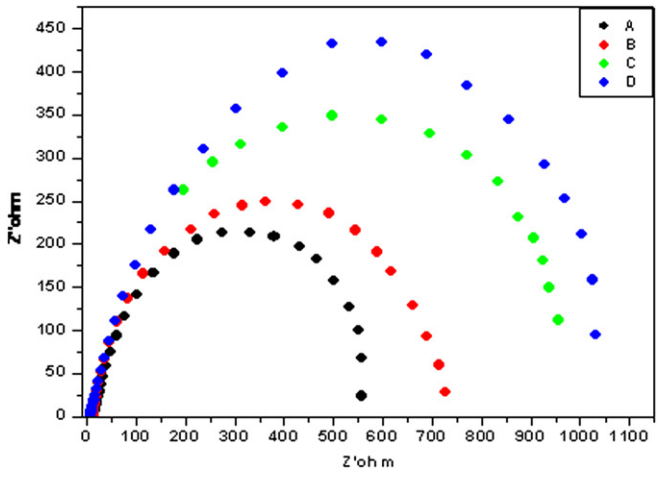

Fig. 9. Nyquist plots (Z'' vs Z') obtained for Ni–W alloy deposit and for various amounts of TiO_2 incorporated in to Ni–W alloy deposit by PC Method.

Table 5
Parameters derived from electrochemical impedance spectrum of Ni–W deposit and Ni–W–TiO_2 nanocomposite coatings obtained using DC Method.

Deposit	TiO_2 in the deposit (wt%)	R_{ct} (Ω cm^2)	C_{dl} (μF cm^{-2})
A	0	454	124.90
B	1.1	643	88.44
C	2.2	877	60.52
D	3.3	980	56.02

Table 6
Parameters derived from electrochemical impedance spectrum of Ni–W deposit and Ni–W–TiO_2 nanocomposite coatings obtained using PC Method.

Deposit	TiO_2 in the deposit (wt%)	R_{ct} (Ω cm^2)	C_{dl} (μF cm^{-2})
A	0	557	103.21
B	1.9	726	78.33
C	3.7	957	55.46
D	5.6	1032	47.24

where, i_{corr} is the corrosive current density. b_a and b_c are the respective anodic and cathodic Tafel slopes. R_{ct} is charge transfer resistance. In otherwords, $i_{corr} = (K/R_{ct})$. Incorporation of TiO_2 increased R_{ct} values suggesting decrease in corrosion current density values (i_{corr}).

Corrosion of electrodeposits in 3.5% NaCl solution involved electrochemical reactions. Usually noble metal coatings offer a barrier protection to steel [42]. In the present study, Ni–W alloy deposit was found to contain $Ni_{17}W_3$ intermetallic phase. This phase was nobler than nickel. Nickel dissolved from the alloy matrix by galvanic action. Ni–W–TiO_2 composite surface was found to be smooth and covered by smaller spherical crystallites. Thus TiO_2 incorporation prevented the dissolution of nickel by adsorbing on the anodic sites.

The observed semicircle in the Nyquist plots for both DC and PC electrodeposits suggested a simple RC circuit. The addition of TiO_2 in the deposit decreased the capacitance of the double layer values. Pulse current deposits had smaller crystallites and provided larger surface area. It resulted in decrease of double layer capacitance compared to those obtained for DC deposits.

4. Conclusions

Ni–W alloy and Ni–W–TiO_2 nanocomposite coatings on mild steel were prepared by pulse current electrodeposition. Thus prepared nanocomposite coating was compared with those prepared by direct current electrodeposition. Ni–W alloy coating surface was found to be covered by long needle like crystals while Ni–W–TiO_2 composites coating surface had smaller spherical grains. Incorporation of TiO_2 particles in Ni–W alloy coating increased the microhardness values. Ni–W alloy deposit was found to have $Ni_{17}W_3$ intermetallic phase which was nobler than nickel. Dissolution of nickel was hindered by the incorporation TiO_2 in the Ni–W alloy deposit. The pulse current electrodeposited nanocomposite coatings had enhanced corrosion resistance compared to those of direct current electrodeposition.

Acknowledgments

The authors thank CSIR, New Delhi for awarding CSIR emeritus scientist scheme and acknowledge Head of the department of Physics, Alagappa University, Karaikudi for the assistance in XRD measurements.

References

[1] S. Mirzamohammadi, R. Kiarasi, M.K. Aliov, A.R. Sabur, A. Hassanzadeh-Tabrizi, Study of corrosion resistance and nanostructure for tertiary Al2O3/Y_2O_3/CNT pulse electrodeposited Ni based nanocomposite, Transactions of the Institute of Metal Finishing 88 (2) (2010) 93–99.

[2] N Imaz, E Garcia-Lecina, J.A Diez, Corrosion properties of double layer nickel coatings obtained by pulse plating techniques, Transactions of the Institute of Metal Finishing 88 (5) (2010) 256–261.

[3] N.S Qu, D Zhu, K.C Chan, W.N Lei, Pulse electrodeposition of nanocrystalline nickel using ultra narrow pulse width and high peak current density, Surface and Coatings Technology 168 (2003) 123–128.

[4] T Song, D.Y Li, Tribological, mechanical and electrochemical properties of nanocrystalline copper deposits produced by pulse electro-deposition, Nanotechnology 17 (2006) 65–78.

[5] T Borkar, S.P Harimkar, Effect of electrodeposition conditions and reinforcement content on microstructure and tribological properties of nickel composite coatings, Surface and Coatings Technology 205 (2011) 4124–4134.

[6] M.A Khazrayie, A.R.S Aghdam, Si_3N_4/Ni nanocomposite formed by electroplating: effect of average size of nanoparticulates, Transactions of Nonferrous Metals Society of China 20 (2010) 1017–1023.

[7] F. Xia, M. Wu, F. Wang, Z. Jia, A. Wang, Nanocomposite Ni–TiN coatings prepared by ultrasonic electrodeposition, Current Applied Physics 9 (2009) 44–47.

[8] L.M Chang, J.H Liu, R.J Zhang, Corrosion behavior of electrodeposited Ni/Al_2O_3 composite coating covered with a NaCl salt film at 800 C, Materials and Corrosion 9999 (2010) 1–6.

[9] H. Hasannejad, T. Shahrabi, M. Jafarian, A.S. Rouhaghdam, EIS study of nanocrystalline Ni–cerium oxide coating electrodeposition mechanism, Journal of Alloys and Compounds 509 (2011) 1924–1930.

[10 Ikram ul Haq, Tahir I. Khan, Tribological behavior of electrodeposited Ni–SnO_2 nanocomposite coatings on steel, Surface and Coatings Technology 205 (2011) 2871–2875.

[11] S. Ramalingam, V.S. Muralidharan, A. Subramania, Electrodeposition and characterization of Cu–TiO_2 nanocomposite coatings, Journal of Solid State Electrochemistry 13 (2009) 1777–1783.

[12] A. Gomes, M.I. da Silva Pereira, M.H. Mendonc, F.M. Costa, Zn–TiO_2 composiote films prepared by pulse electrodeposition, Journal of Solid State Electrochemistry 9 (2005) 190–196.

[13] Seishiro Ito, Takenori Deguchi, Kiyohisa Imai, Mitsunobu Iwasaki, Hiroaki Tada, Preparation of highly photocatalytic nanocomposite films consisting of TiO_2 Particles and Zn electrodeposited on steel, Electrochemical and Solid-State Letters 2 (9) (1999) 440–442.

[14] P. Baghery, M. Farzam, A.B. Mousavi, M. Hosseini, Ni–TiO_2 nanocomposite coating with high resistance to corrosion and wear, Surface and Coatings Technology 204 (2010) 3804–3810.

[15] Weiwei Chen, Yedong He, Wei Gao, Electrodeposition of sol-enhanced nanostructured Ni–TiO_2 composite coatings, Surface and Coatings Technology 204 (2010) 2487–2492.

[16] Xiao-kui Yang, Qing Li, Jun-ying Hu, Xian-kang Zhong, Shi-yan Zhang, The electrochemical corrosion behavior of sealed Ni–TiO_2 composite coating for sintered NdFeB magnet, Journal of Applied Electrochemistry 40 (2010) 39–47.

[17] S.A. Lajevardi, T. Shahrabi, V. Hasannaeimi, Synthesis and mechanical properties of nickel–titania composite coatings, Materials and Corrosion 62 (2011) 29–34.

[18] S. Spanou, E.A. Pavlatou, N. Spyrellis, Ni/nano TiO_2 composite electrodeposits: textural and structural modifications, Electrochimica Acta 54 (2009) 2547–2555.

[19] J. Li, Y. Sun, X. Sun, J. Qiao, Mechanical and corrosion-resistance performance of electrodeposited titania–nickel nanocomposite coatings, Surface and Coatings Technology 192 (2005) 331–335.

[20] G. Parida, D. Chaira, M. Chopkar, A. Basu, Synthesis and characterization of Ni–TiO_2 composite coating by electro-co-deposition, Surface and Coatings Technology 205 (2011) 4871–4879.

[21] A. Chianpairot, G. Lothongkum, C.A. Schuh, Y. Boonyongmaneert, Corrosion of nanocrystalline Ni–W alloys in alkaline and acidic 3.4 wt% NaCl solutions, Corrosion Science 53 (2011) 1066–1071.

[22] K.R. Sriraman, S. Ganesh Sundara Raman, S.K. Seshadri, Corrosion behavior of electrodeposited nanocrystalline Ni–W and Ni–Fe–W alloys, Materials Science and Engineering A 460–461 (2007) 39–45.

[23] M. Zemanova, M. Krivosudska, M. Chovancova, V. Jorık, Pulse current electrodeposition and corrosion properties of Ni–W alloy coatings, Journal of Applied Electrochemistry 41 (2011) 1077–1085.

[25] S. Kabi, K. Raeissi, A. Saatchi, Effect of polarization type on properties of Ni–W nanocrystalline electrodeposits, Journal of Applied Electrochemistry 39 (2009) 1279–1285.

[26] M.D. Obradovic, G.Z. Bosnjakov, R.M. Stevanovic, M.D. Maksimovic, A.R. Despic, Pulse and direct current plating of Ni–W alloys from ammonia–citrate electrolyte, Surface and Coatings Technology 200 (2006) 4201–4207.

[27] M. Momenzadeh, S. Sanjabi, The effect of TiO_2 nanoparticle co-deposition on microstructure and corrosion resistance of electroless Ni–P coating, Materials and Corrosion 62 (2011) 1–6.

[28] L.M. Chang, M.Z. An, S.Y. Shi, Microstructure and characterization of Ni–Co/Al_2O_3 composite coating by pulse reversal electrodeposit, Materials Chemistry and Physics 100 (2006) 395–399.

[29] L.M. Chang, H.F. Guo, M.Z. An, Electrodeposition of Ni–Co/Al_2O_3 composite coating by pulse reverse method under ultrasonic condition, Materials Letters 62 (2008) 3313–3315.

[30] B. Ranjith, G. Paruthimal Kalaignan, Ni–Co/TiO_2 nanocomposite coating prepared by pulse and pulse reversal methods using acetate bath, Applied Surface Science 257 (2010) 42–47.

[31] Y. Yao, S. Yao, L. Zhang, H. Wang, Electrodeposition and mechanical and corrosion resistance properties of Ni–W/SiC nanocomposite coatings, Materials Letters 61 (2007) 67–70.

[32] H. Baolei, L. Xinchun, Effect of La_2O_3 on microstructure, mechanical andtribological properties of Ni–W coatings, Chinese Science Bulletin 54 (2009) 4566–4570.

[33] B. Han, X. Lu, Effect of nano-sized CeF_3 on microstructure, mechanical, high temperature friction and corrosion behavior of Ni–W composite coatings, Surface and Coatings Technology 203 (2009) 3656–3660.

[34] K. Hsu Hou, Y. Cheng Chen, Preparation and wear resistance of pulse electrodeposited Ni–W/Al_2O_3 composite coatings, Applied Surface Science 257 (2011) 6340–6346.

[35] M.F. Cardinal, P.A. Castro, J. Baxi, H. Liang, F.J. Williams, Characterization and frictional behavior of nanostructured Ni–W–MoS_2 composite coatings, Surface and Coatings Technology 204 (2009) 85–90.

[36] M. Aliofkhazraei, Sh. Ahangarani, A. Sabour Rouhaghdam, Effect of the duty cycle of pulsed current on nanocomposite layers formed by pulsed electrodeposition, Rare Metals 29 (2) (2010) 209–213.

[37] Baolei Han, Xinchun Lu, Tribological and anti-corrosion properties of Ni–W–CeO_2 coatings against molten glass, Surface and Coatings Technology 202 (2008) 3251–3256.

[38] B.D. Cullity, S.R. Stock, S. Stock, Elements of X-ray Diffraction Fraction, Addison-Wesley, London, 2001.

[39] S. Kyu Kim, H. Jae Yoo, Formation of bilayer Ni–SiC composite coating by electrodeposition, Surface and Coatings Technology 108–109 (1998) 564–569.

[40] K.H.W. Seah, M. Krishna, V.T. Vijayalakshmi, J. Uchil, Corrosion behavior of garnet particulate reinforced LM13 Al alloy MMCs, Corrosion Science 44 (2002) 917–925.

[41] M. Stern, The mechanism of passivating-type inhibitors, Journal of the Electrochemical Society 105 (1958) 638–647.

[42] W.H Ailor, Hand Book on Corrosion Testing and Evaluation, John Wiley and sons, NewYork, Inc, 1971.